

# 1      **Microscopic Characteristics of Biodiesel – Graphene Oxide Nanoparticle** 2      **Blends and their Utilisation in a Compression Ignition Engine**

3                      S. Nagaraja<sup>1\*</sup>, D. Dsilva Winfred Rufuss<sup>2</sup>, A. K. Hossain<sup>3</sup>

4  
5      <sup>1</sup>Department of Mechanical Engineering, Akshaya College of Engineering and Technology, Coimbatore, India.

6      <sup>2</sup>Department of Thermal and Energy Engineering, School of Mechanical Engineering, Vellore Institute of  
7                      Technology (VIT), Vellore-632014, Tamil Nadu, India.

8      <sup>3</sup>Aston Institute of Materials Research (AIMR), School of Engineering and Applied Science, Aston University,  
9                      Aston Triangle, Birmingham B4 7ET, UK.

10                      \*Corresponding author (S. Nagaraja): nagarajacit@yahoo.com

## 11 12      **Abstract**

13      Use of nano-additives in biofuels is an important R&D topic for achieving optimum engine  
14      performance with reduced emissions. In this study, rice bran oil was converted into biodiesel  
15      and graphene oxide (GO) nanoparticles were infused into biodiesel-diesel blends. Two blends  
16      containing (i) 5% biodiesel, 95% diesel and 30 ppm GO (B5D95GO30) and (ii) 15%  
17      biodiesel, 85% diesel and 30 ppm GO (B15D85GO30) were prepared. The fuel properties  
18      like heating value, kinematic viscosity, cetane number, etc. of the nanoadditives–biodiesel-  
19      diesel blends (NBDB) were measured. Effects of injection timing (IT) on the performance,  
20      combustion and emission characteristics were studied. It was observed that both  
21      B15D85GO30 and B5D95GO30 blends at IT23° gave up to 13.5% reduction in specific fuel  
22      consumption. Compared to diesel, the brake thermal efficiency was increased by 7.62% for  
23      B15D85GO30 at IT23° and IT25°. An increase in IT from 23° to 25° deteriorated the  
24      indicated thermal efficiency by 6.68% for B15D85GO30. At maximum load condition, the  
25      peak heat release rates of NBDB were found to be lower than the pure diesel at both IT. The  
26      CO, CO<sub>2</sub> & NO<sub>x</sub> emissions were reduced by 2-8%. The study concluded that B15D85GO30  
27      at IT23° gave optimum results in terms of performance, combustion and emission  
28      characteristics.

## 29 30 31      **Keywords**

32      Combustion; Emission; Graphene oxide; Injection timing; Performance; Rice bran biodiesel

## Nomenclature

B0	Pure diesel (0% biodiesel)
B15D85GO30	15% biodiesel, 85% diesel and 20 ppm GO
B5D95GO30	5% biodiesel, 95% diesel and 30 ppm GO
BDB	Bio-diesel blends
BSFC	Brake specific fuel consumption
bTDC	Before top dead centre
BTE	Brake thermal efficiency
CNT	Carbon nanotubes
CA	Crank angle
CI	Compression ignition
COOH	Carboxylic acid
CR	Compression ratio
E5	Engine test express software
EG	Exhaust gas
EGT	Exhaust gas temperature
GNP	Graphene nano-platelets
GO	Graphene oxide
GO-BDB	Graphene oxide biodiesel blends
GONP	Graphene oxide nanoparticle
HRR	Heat release rate
IMEP	Indicated mean effective pressure
IT	Injection timings
ITE	Indicated thermal efficiency
JCPDS	Joint committee on powder diffraction standards
MWCNT	Multiwalled carbon nanotubes
NBDB	Nano additives – biodiesel - diesel blends
NP	Nano-particles
OH	Hydroxyl group
PM	Particulate matter
PME	Pongamia methyl ester
SEM	Scanning electron microscope
TEM	Transmission electron microscope
UHC	Unburnt hydrocarbon
VCR	Variable compression ratio
XRD	X-ray diffraction

## 34 **1. Introduction**

35 Biodiesel is considered to be a suitable replacement for pure diesel for using in the  
36 compression ignition (CI) engines. This biodiesel can be extracted from various feedstock  
37 such as vegetable oil, animal fats, non-edible oils [1]. Used cooking oil is one of the  
38 commonly used feedstocks which can be converted into high-quality biodiesel [2]. The use of  
39 non-waste based feedstock such as blends of hazelnut oil and rapeseed oil biodiesels were  
40 also investigated by the researcher [3]. However, the biodiesel application in compression  
41 ignition (CI) engines is hindered by some drawbacks such as higher viscosity, higher density,  
42 lower cloud point, inefficient fuel atomization, and higher NO<sub>x</sub> emissions [1,4,5]. To  
43 overcome these drawbacks, some of the techniques investigated by the researchers are (i) use  
44 of fuel additives, (ii) use of hybrid fuels, and (iii) engine parameters modifications. One such  
45 technique is the inclusion of nano-particles additives with bio-diesel blends (BDB) [2].  
46 Literature reported that nano-additives improved thermo-physical properties, performance  
47 characteristics (specific fuel consumption, brake power, etc.) [6], and combustion  
48 characteristics such as heat release rate (HRR) [7–10] of the pure diesel fuel. The  
49 performance and emission characteristic of the engine depends on the type and amount of  
50 nano-additives, and engine parameters (injection timing, injection pressure, compression  
51 ratio, etc.) [11–14]. The following literature investigated the behavioural variations of  
52 commonly used nano-particles (aluminium oxide, iron, and cerium oxide) and recently  
53 evolved nano-particles like graphene oxides and carbon nanotubes (CNT) when added to  
54 biofuels.

55 Adding the metal oxides of aluminium, titanium, silicon, etc. with biodiesel increases the  
56 thermo-physical properties (viscosity, cetane number and heating value) and helps in  
57 augmenting the thermal efficiency with the reduction in brake specific fuel consumption  
58 (BSFC) as compared to the fossil diesel fuel [15,16]. The Al<sub>2</sub>O<sub>3</sub> nanoparticles mixed with  
59 water (nano-fluids) was added to fossil diesel and tested in a diesel engine [14]. The authors  
60 reported that the additives improved the brake thermal efficiency (BTE) by 5.5% with a  
61 significant reduction in exhaust gas emissions [17]. Another study reported that Al<sub>2</sub>O<sub>3</sub>  
62 nanoparticle mixed with honge oil methyl ester improved the BTE by 10% with 11%  
63 reduction in BSFC. Also, the HC and CO emissions were dwindled by 26% and 43%  
64 respectively [18]. Also, it is inferred from the same study that increasing the blending ratio of  
65 nanoparticles more than 60 ppm reduces the fuel stability of the NBDB [18]. The aluminium

66 oxide, boron oxide and iron nano-additives were added separately to diesel fuel; the study  
67 found that at higher loads, the peak combustion pressure and BSFC were reduced when  
68 compared to the pure diesel operation [19]. An increase in BTE was observed when  
69 aluminium oxide nano-particles were added with Mahua BDB [20,21]. An improvement in  
70 the HRR was reported when  $Al_2O_3$  nanoparticles were added in biodiesel-diesel blends [7].  
71 Compared to pure diesel operation, a notable enhancement in the BTE (about 12%) was  
72 reported when aluminium oxide and cerium oxide nanoparticles were added with biodiesel-  
73 diesel blends [20]. The authors have reported that nano-additives gave up to 30% and 38%  
74 decrease in the CO and HC gas emissions as compared to pure diesel. They recommended  
75 that the effects of other engine parameters like ignition timing, injection pressure should be  
76 investigated in the near future with various nanoparticles-biodiesel blends [20].

77 The injection timings and injection pressure play an essential role in determining the  
78 combustion characteristics of the NBDB [22]. The performance characteristic of a diesel  
79 engine was improved by adding pentanol and titanium oxides nano-additives individually  
80 with corn biodiesel. The effect of injection pressure was investigated and it was inferred that  
81 the additives improved the BTE to the engine and reduced the  $CO_2$  and  $NO_x$  emissions [23].  
82 However, the effects of injection timings were not investigated by the authors. Three  
83 different nanoparticles titanium dioxide, copper nitrate and cerium acetate were added  
84 separately to pure diesel and their combustion and emission characteristics were analysed  
85 [24]. The authors found that there was a reduction in the sound level of the engine block  
86 leading to the effective control of vibration [24]. Cerium oxide ( $CeO_2$ ) was added with  
87 pongamia methyl ester (PME), it was inferred that the  $CeO_2$  expedites the procedure of  
88 burning because of its high surface: volume ratio [8]. Another study reported that compared  
89 to  $CeO_2$  nanoparticles, cerium composite oxide ( $Ce_{0.5}Co_{0.5}$ ) reduced a higher amount of CO,  
90  $NO_x$  and UBHC emissions when blended with waste cooking oil [25]. Titanium oxide  
91 nanoparticles were diffused with palm oil biodiesel-diesel blends to reduce the BSFC and  
92 downturn the exhaust gas emissions like HC and CO. The study found that at part-load  
93 conditions, the nitrates of oxygen can be significantly decreased with the use of exhaust gas  
94 recirculation [26].

95 Recently, studies investigated the effect of various injection timing in nanoparticle enhanced  
96 BDB [9]. Nickel oxide was chosen as the nanoparticle and the effect of three injection  
97 timings ( $23^\circ bTDC$ ,  $19^\circ bTDC$  and  $27^\circ bTDC$ ) on the behavioral characteristics were

98 investigated. The authors reported that advancing the injection timing (to IT27°) improved  
99 the HRR and BTE of the engine. From the above literature review, it can be summarised that  
100 the traditional nanoparticle impregnation with biodiesel improves the combustion and  
101 performance characteristics with a considerable curtailment in the exhaust emissions.  
102 Recently, nano-additives such as graphene, carbon nanotubes are being investigated by the  
103 researchers due to their better physicochemical properties. However, hardly any literature  
104 was available pertaining to GO and CNT impregnation with biodiesel.

105 The effects of GO enhancement with dairy scum oil in the concentration of 20-60 ppm  
106 revealed that the BTE was improved by 12%; BSFC, UBHC emission, smoke emission and  
107 CO were reduced by 9%, 21%, 24%, and 39% respectively. Better HRR and peak in-cylinder  
108 pressures were achieved for the nanoparticle-biodiesel blends as compared to pure biodiesel  
109 [10]. Graphene quantum dots increased the torque and power output of the engine by 12%  
110 and 28% respectively when fueled with ethanol-biodiesel blends, with a considerable  
111 reduction (about 14%) in BSFC. The authors observed a significant reduction (about 30%) in  
112 the CO and HC emissions as compared to pure diesel operation [27]. Multi-walled carbon  
113 nanotube was mixed with jatropha biodiesel in various concentrations between 10-50 mg/l, a  
114 16% improvement in BTE and 15% reduction in BSFC were observed for blended biodiesel  
115 as compared to pure biodiesel operation. Furthermore, the authors reported that  
116 approximately 50% reduction in the CO and UBHC were observed for the CNT blended  
117 biodiesel when compared to virgin biodiesel [28]. Another literature reported that as  
118 compared to neat biodiesel, the brake power was considerably increased when graphene  
119 oxide and CNT were impregnated in camelina oil biodiesel [29]. They reported that the UHC  
120 and CO emissions were significantly reduced, NO<sub>x</sub> emission was slightly increased [29].  
121 Compared to neat biodiesel operation, the BTE was increased by 17% when graphene oxide  
122 was added to jatropha methyl ester [30]. The HRR and in-cylinder pressure were increased by  
123 6% and 8% respectively. The authors reported that compared to neat biodiesel operation, the  
124 nano-additive blends gave reduced CO, UHC and NO<sub>x</sub> emissions by 60%, 50% and 15%  
125 respectively [30]. Another study carried out by the same authors reported that the graphene  
126 nanoparticles' impregnation in jatropha methyl ester reduced BSFC by 20% as compared to  
127 neat biodiesel [31].

128 The BSFC was decreased by 35% when a nano-additive fuel blend was used in the diesel  
129 engine consisting a mixture of GO, multi-walled carbon nanotubes (MWCNTs), n-butanol

130 and jatropha methyl ester [32]. The CO, NO<sub>x</sub> and UBHC emissions were reduced by 55%,  
 131 50% and 45% respectively [32]. The GO was impregnated with *Ailanthus altissima* biodiesel  
 132 blends at various concentrations (30 ppm, 90 ppm); the authors have inferred that the BP and  
 133 EGT were considerably increased, whereas BSFC and oxides of carbon and nitrogen were  
 134 significantly decreased [33]. Table 1 shows a summary of various nano-additives used with  
 135 biodiesel. The GO and CNT nano-additives blended with biodiesel gave a better performance  
 136 with a minimum emission as compared to unblended biodiesel (Table 1). However,  
 137 researchers have used mostly *Jatropha* oil as a major biodiesel source for nano-additive  
 138 blends with biodiesel. Nevertheless, recently evolved biodiesel such as rice bran biodiesel,  
 139 leaf (*veronica fordii*) biodiesel, yolk biodiesel were not being investigated with GO and CNT  
 140 nano-additives yet. In addition, researchers suggested that in terms of the biodiesel yield  
 141 quantity, rice bran and leaf oil has better potential when compared to *jatropha* oil [34–36].

142 Table 1. Summary of the previous research work on nano-additives - biodiesel blends

Reference	Nanoparticles added with BDB	Inference
[7]	Aluminium oxide	BTE and heat release rate increased.
[9]	Nickel oxide	HRR and BTE improved. BSFC decreased.
[10]	Graphene oxide	BTE improved by 12%. BSFC reduced by 9%.
[15]	Aluminium oxide, titanium oxide and silicon oxide	BTE increased and BSFC decreased. CO emission reduced.
[18]	Aluminium oxide	BTE increased by 10%. BSFC, HC emissions, CO emissions reduced by 11%, 26% and 43% respectively.
[19]	Aluminium oxide, boron oxide and iron	Peak in-cylinder pressure and SFC deteriorated at high loads.
[20]	Aluminium oxide and cerium oxide nanoparticles	BTE improved by 12%. NO, CO, HC and smoke emissions decreased by 30%, 60%, 44% and 38%.
[21]	Aluminium oxide and cerium Oxide	BTE improved by 3% NO <sub>x</sub> emission reduced by 4%
[23]	Pentanol and titanium oxides	BTE improved CO <sub>2</sub> and NO <sub>x</sub> emissions decreased.

[24]	Titanium dioxide, copper nitrate and cerium acetate nano-additives used separately	CO and HC emissions reduced. Cerium acetate gave better results than other nano-additives.
[25]	CeO <sub>2</sub> and Ce <sub>0.5</sub> Co <sub>0.5</sub>	CO emission reduced by 39%. UBHC reduced by 40%
[26]	Titanium oxide	CO emission decreased by 46%. NO <sub>x</sub> reduced by 20% when EGR was used.
[27]	Graphene quantum dot	Power increased by 28%. CO and HC emissions reduced by 30%.
[29]	Graphene oxide and CNT	Brake power and BSFC increased. HC, CO emissions decreased, NO increased.
[30]	Graphene oxide	BTE, HRR and in-cylinder pressure increased by 17%, 6% and 8% respectively.
[31]	Graphene oxide	BSFC decreased by 20%; CO, NO decreased by 40%.
[32]	Graphene oxide, MWCNTs	Peak in-cylinder pressure increased by 6%. BSFC decreased by 35%.
[33]	Graphene oxide	Brake power increased. BSFC decreased. CO, NO gas emissions decreased.

143 Furthermore, it is construed from the literature review that none of the studies investigated  
144 the effects of injection timing on the GO nanoparticle enhanced BDB. To bridge the above  
145 research gap, the present research focusses on incorporating recently evolved nanoparticles  
146 i.e. GO with rice bran biodiesel-diesel blends and investigate the performance, combustion  
147 and emission characteristics of the engine. The eminent combination at optimum injection  
148 timing of nano additives-biodiesel blends has a higher aptitude to become a potential  
149 substitute for fossil diesel. The objectives of the current study are: (i) to investigate the  
150 microscopic characteristics of the rice bran biodiesel-diesel-nanoparticle blends, (ii) To  
151 optimize the injection timing with the best combination of nano additives – biodiesel - diesel  
152 blends (NBDB), (iii) To reduce the exhaust emission level and improve the combustion and  
153 performance characteristics of NBDB, and (iv) comparison of the combustion and exhaust  
154 emission results with and without nano additives.

## 155 2. Materials and Methods

### 156 2.1. Production of biodiesel

157 The unprocessed rice bran oil was stirred at 1000 rpm and heated up to 70°C. Then, KOH and  
158 methanol were mixed and the raw heated oil was added to the mixture. Rice bran oil,

159 methanol, and KOH were mixed at the ratio of 1000ml: 250ml: 5g respectively [13,37]. Due  
160 to the density variations, methyl ester was settled at the top of the mixture and separated. The  
161 biodiesel was then washed with preheated water and filtered [38]. This distillation process  
162 was repeated until the desired purity of the biodiesel was obtained.

## 163 **2.2. Preparation of GO enhanced biodiesel-diesel blends**

164 Graphene oxide was purchased from SRL, India with the specified purity of about 99.7%, the  
165 GO was added to the prepared BDB following the procedure adopted in the literature [39].  
166 The particle size, surface area and thermal conductivity of the GO nanoparticle are 22.5-26  
167 nm, 492 m<sup>2</sup>/g, and 3000 W/mK respectively. Various combinations of nanoparticle-diesel-  
168 biodiesel blends (B5D95GO30 – 5% biodiesel, 95% diesel and 30 ppm GO; B15D85GO30 -  
169 15% biodiesel, 85% diesel and 30 ppm GO) were prepared using an ultrasonic shaker for  
170 homogeneous dispersion of nano-additives. The main challenge faced during the preparation  
171 of GO enhanced biodiesel-diesel blend was maintaining the stability of the nanocomposite  
172 blend. The stability of the nanocomposites is influenced by agglomeration and clogging of  
173 nanoparticle in the base fluid due to Vander walls interactions [40,41]. The stability of  
174 NDBDs was ensured by adopting the two-step stability process suggested in the literature  
175 [42–44], they include (i) choosing the small particle size with less weight in the colloidal  
176 solution which reduces the possibility of getting agglomerated over the base fluid, and  
177 followed by (ii) continuous agitation (in an ultrasonic shaker) with the addition of surfactant  
178 [Sodium Dodecyl Benzene Sulfonate (SDBS)] which reduces the probability of nanoparticles  
179 getting coagulated over the base material. The above two steps were followed in the present  
180 research to ensure the stability of the nanocomposites thus reassuring the homogeneous  
181 dispersion of nanoparticles on the biodiesel blends. Once the NBDBs were prepared, their  
182 properties were measured. The technical details of the engine, instrumentations and various  
183 equipment used for measuring fuel properties are shown in Tables 2 and Table 3.

## 184 **2.3. Experimental setup**

185 The engine test was conducted using a single-cylinder, four-stroke diesel engine. The rated  
186 power output of the engine is 3.7 kW, the engine was operated at constant speed mode with  
187 varying injection timing (23° & 25° bTDC) and load (0 - 100 Nm). At first, the engine was  
188 started with pure diesel (B0) and then switched to GO-BDB fuels (B5D95GO30 and  
189 B15D85GO30). The detailed specification of the engine is given in Table 4. Fig. 1 presents



190 schematic of the test rigs showing two fuel tanks (one for GO-BDB fuels and one for diesel  
 191 fuel), air box, manometer, fuel measuring unit, transmitters for air and fuel flow  
 192 measurements, process indicator and engine indicator. Eddy current dynamometer to apply  
 193 and vary the load on the engine. NETEL gas analyser was used to measure the concentration  
 194 of CO, HC, CO<sub>2</sub>, NO<sub>x</sub> gases in the exhaust stream.

195 Table 2. Technical details and measurement accuracies of the instruments

<b>Equipment</b>	<b>Make &amp; Model</b>	<b>Range and Accuracy</b>	<b>Parameter</b>
CI Engine	Kirloskar, TV1, CVCRO3-OECU	CR range: 12 to 20, CR accuracy: ±0.1mm	Performance, Combustion
Crank Angle sensor	Kubler (Germany), Model - 8.3700.1321.0360	Resolution: 1 degree, 2048 steps (11-Bit)	Crank angle position
Air intake measurement	DP sensor with inline transmitter	Pressure Transmitter Range: 250 mmwc (millimeter water column)	Air intake flow
Fuel meter	Yokogawa, Model - EJA110-EMS-5A- 92NN	Calibration range:0-500 mm H <sub>2</sub> O	Fuel flow
Load indicator	Selectron, Model-PIC 152- B2, 85 to 270 VAC	Re-transmission output 4-20 mA	
Eddy current dynamometer	Saj Test Plant Ltd., AG 10		Engine load
Load cell	Sensortronics 60001	Zero Balance ± 0.1 mV/V Non linearity < ± 0.025% Hysteresis < ± 0.020% Non-repeatability < ± 0.010%	
Temperature sensor	Wika, Model: T19.10.3K0- 4NK-Z, K type Thermocouple, Output 4-20 mA, Supply 24 VDC	Calibrated for range 0 - 1200°C	Temperature
Pressure sensor	PCB Piezotronics, M111A22 Piezo-electric: 0-100 bar	Resolution: 0.1 psi Sensitivity: 1 mV/psi Low Frequency Response (5%): 0.001 Hz Linearity: 2% (Best Straight Line)	In-cylinder pressure
Rotameter	Eureka, PG 6, Range: 40-400 LPH	Accuracy: ±2% of Full Flow Standard	Water flow

196

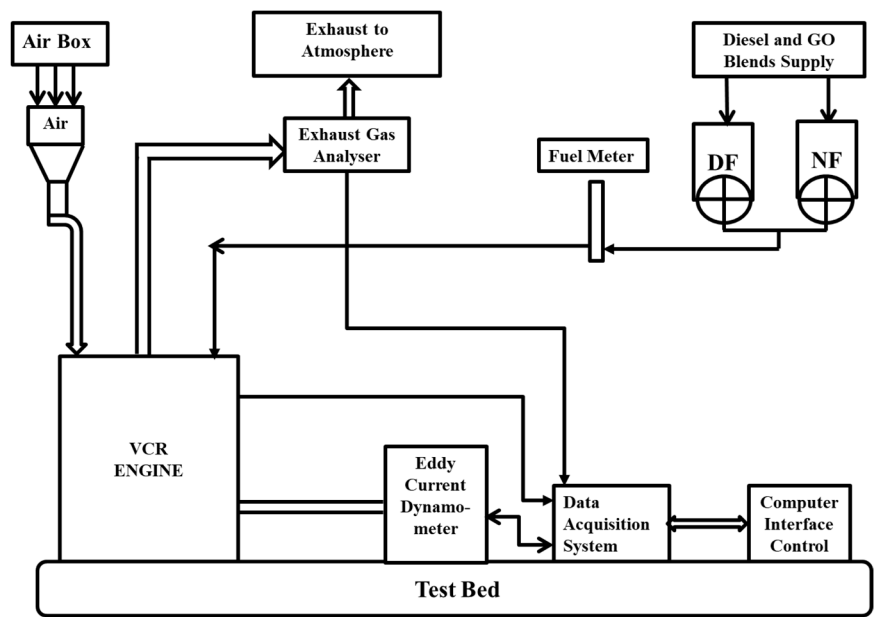
197

Table 3. Technical details of the equipment used for fuel preparation and properties

Name of the apparatus	Model	Accuracy	Parameter
Ultrasonic m/c	Johnson Plastasonic, ULP-3000	$\pm 0.01^\circ$	Preparation of nano-additive blends
Kinematic viscometer	Biolab Model – Viscol 10a	Range: 0.5 - 25000 cSt, Accuracy: $\pm 0.02$ cSt	Kinematic viscosity
Hydrometer	Thomas scientific Model – 6025C47	Range: 0.790-0.900 g/cm <sup>3</sup> Accuracy: $\pm 0.001$	Density
Bomb Calorimeter	Orbit Technologies, Model – 6100	Precision: 0.1 - 0.2% Temp resolution: 0.0001°C	Heating value
Pensky-Martens flash point tester	Pensky-Martens, Model - PMA 500	Range: 20 - 410 °C Heating rate: 0.5 to 12 °C/min.	Flash and fire point

198 The specification of the gas analyser is shown in Table 5. Combustion analysis was done by a  
 199 transducer (quartz piezoelectric pressure transducer) placed on the cylinder head and a crank  
 200 angle encoder fixed on the output shaft of the engine. Combustion parameters such as in-  
 201 cylinder pressure, occurrences of peak in-cylinder pressures, ignition delay and heat release  
 202 rate were obtained and analysed using LabVIEW based software and engine test express (E5)  
 203 software. The E5 software was developed by Legion Brothers exclusively to investigate the  
 204 characteristics variation of an engine.

205



206

207

Fig. 1. Schematic diagram of the experimental setup

Table 4. Specification of the experimental engine

Manufacturer and Type	Kirloskar, single-cylinder, water-cooled
No. of strokes	Four
Rated Power	3.7 KW
Bore/Stroke	87.5 mm / 110 mm
Rated RPM	1500
Compression Ratio	17.5 (standard)
Injection Timing	21 to 25 ° bTDC
Type of ignition	Compression Ignition
Injection opening pressure	201 bar

Table 5. Technical details of the NETEL (NPM-MGA-2) gas analyser

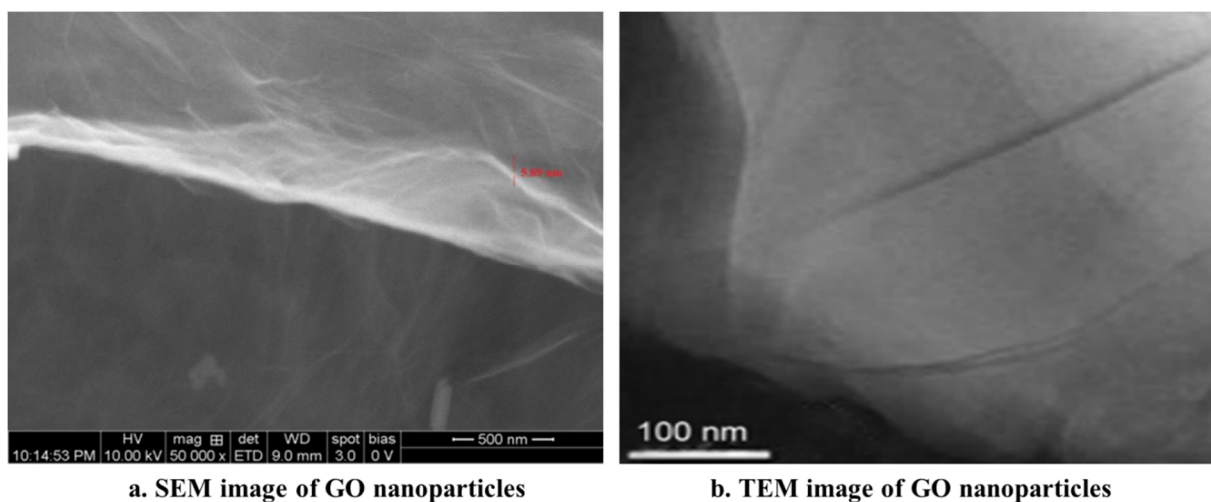
Gas	Range	Resolution
CO	0-10 %	0.01%
CO <sub>2</sub>	0-20 %	0.1%
HC	0-2000 ppm	1 ppm
O <sub>2</sub>	0-25%	0.01%
NO <sub>x</sub>	0-10000 ppm	1 ppm

### 211 3. Results and discussion

#### 212 3.1. Characterisation of GO-BDB fuel

213 The size and range of the nanoparticles are important parameters that affect the dispersion  
 214 efficiency and agglomeration in the derived nano-composites. The surface morphology of GO  
 215 was measured using Carl Zeiss MA15/EVO18 scanning electron microscope and CM-120-  
 216 Philip transmission electron microscope to authenticate the procured GO is in the correct  
 217 nano range. This will aid in the improvement factor of the combustion, performance and  
 218 emission characteristics of blended NBDB as compared to virgin biodiesel owing to the  
 219 quantum effects, expanded surface area and tenability [45–47]. The resolution and  
 220 magnification of the SEM were 3.0 nm and 50-100 K respectively. The operating voltage and  
 221 temperature of TEM lie between 20-100 kV and -100 to 450 °C respectively. The SEM and

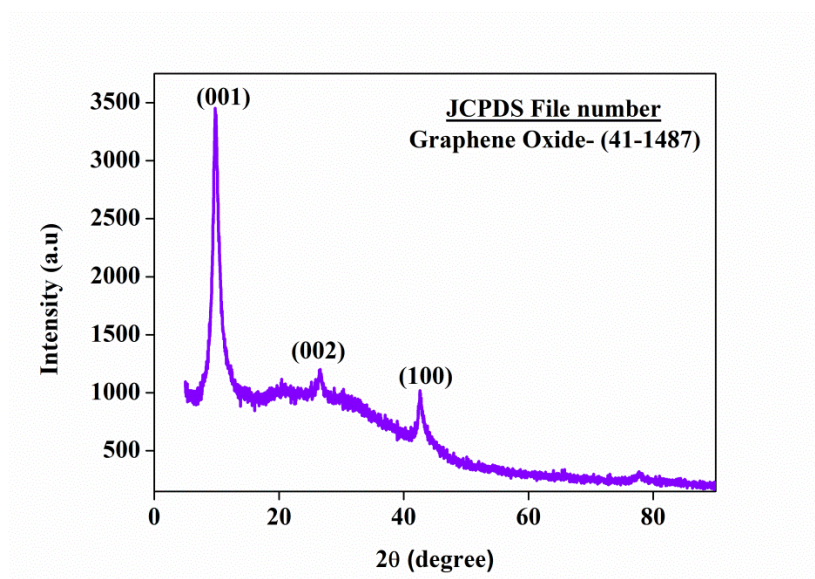
222 TEM images of the GO nanoparticles are depicted in figures Fig. 2 (a) and Fig. 2 (b)  
223 respectively. The size of the nanoparticle was measured using point to point inbuilt  
224 measuring tool and found to be approximately 5.8 nm. The TEM image confirmed a higher  
225 surface to volume ratio which governs the variation in thermal conductivity of the  
226 nanoparticles when dispersed in biodiesel-diesel blends. The phase composition and crystal  
227 structure of the nanoparticle are examined using X-Ray diffraction. Shimadzu diffractometer  
228 (XRD 6000, Japan) with the scattering angle and minimum step angle of about 20 to 80° and  
229 0.002° respectively was used for experimentation. Fig. 3. depicts the XRD pattern of the  
230 graphene oxide nanoparticles.



231

232

Fig. 2. Surface morphology of GO nanoparticle



233

234

Fig. 3. Diffraction pattern confirming the presence of GO

235 The intensive peak ( $2\theta$ ) at  $11.7^\circ$  (hkl plane: 002) is due to the formation of -OH and -COOH  
 236 groups. Due to this character, lattice plane distance decreased and as a result,  $sp^2$  carbon  
 237 (C=C i.e. a carbon atom bonded with two atomic orbital) is re-established. The peak  
 238 corresponding to  $2\theta = 42.6^\circ$  [(hkl plane: 100), JCPDS fl.no: 41-1487] confirms the  
 239 withholding of graphite structure after the reduction process [48].

### 240 3.2. Properties of GO-BDBs

241 The properties such as cetane number, heating value, kinematic viscosity and flash point  
 242 temperatures of the B5D95GO30 and B15D85GO30 blends were measured and compared  
 243 with the fossil diesel and neat biodiesel properties (Table 6). The flash points of pure diesel,  
 244 B5D95GO30 and B15D85GO30 are  $56^\circ\text{C}$ ,  $160^\circ\text{C}$  and  $158^\circ\text{C}$  respectively (Table 6). At  $40^\circ\text{C}$ ,  
 245 the kinematic viscosity of pure diesel was 2.8 cSt; on the other hand, the kinematics viscosity  
 246 of the nano-additive blends was 3.8 cSt. Compared to pure diesel, the heating values of the  
 247 blends were decreased by about 21% (Table 6). The density of the B5D95GO30 and  
 248 B15D85GO30 blends was increased by 6.5% and 7% respectively when compared to the  
 249 density of the pure diesel. The cetane number was measured using the ASTM D613 standard.  
 250 Base fuels (n-hexadecane and 1-methylnaphthalene) were used to calculate the cetane  
 251 number through standard cetane number scale. The required cetane number was calculated  
 252 using the empirical inverse relationship [cetane number = % cetane + 0.15 (% hepta-  
 253 methylnonane)]. The cetane numbers of the GO-BDB were found to be lessened as against  
 254 fossil diesel. The cetane numbers of pure diesel, B5D95GO30 and B15D85GO30 were 46, 42  
 255 and 43 respectively (Table 6).

256 Table 6. Characterisation of GO-BDB fuels

Properties	Measurement Standards	Pure diesel (B0)	Rice-bran biodiesel (B100)	B5D95GO30	B15D85GO30
Flash point temp ( $^\circ\text{C}$ )	D93	56	170	160	158
Kinematic viscosity (cSt) @ $40^\circ\text{C}$	D445	2.8	5.6	3.8	3.8
Lower heating value (MJ/kg)	D4809	46	35	36.23	36.76
Density ( $\text{kg/m}^3$ )	D1298	840	880	865	871
Cetane number	D613 & D976-80	46	42	38	38

### 257 3.3. Performance characteristics

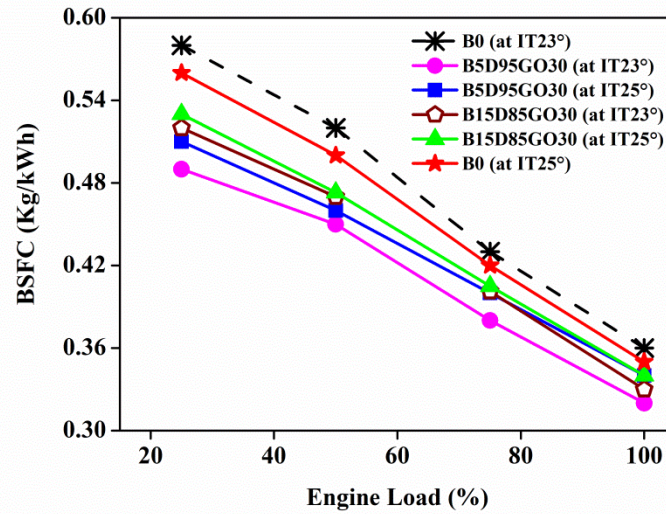
258 The effects of GO-BDBs on engine performance characteristics such as BSFC, BTE, IMEP  
259 and ITE will be discussed in the following sections:

#### 260 3.3.1. Brake Specific Fuel Consumption (BSFC)

261 The BSFC of various fuels with engine load is depicted in Fig. 4. In general, the BSFC of the  
262 B5D95GO30 & B15D85GO30 blends were found to be lower than pure diesel. At IT23°, the  
263 BSFC of the B5D95GO30 fuel was observed to be 11% to 13.5% lower than that of B0 fuel;  
264 whereas, at IT25° the BSFC of the same nano-additive blend was decreased by 3-6% when  
265 compared to B0 fuel (Fig. 4). This proved that advancing injection timing improved BSFC  
266 value in NBDBs. This may be due to the optimistic calorific value, density and viscosity of  
267 GONP; moreover, it acts as an oxygen supporter for biodiesel to yield high pressure and  
268 temperature inside the engine cylinder [7,49].

#### 269 3.3.2. Brake Thermal Efficiency (BTE)

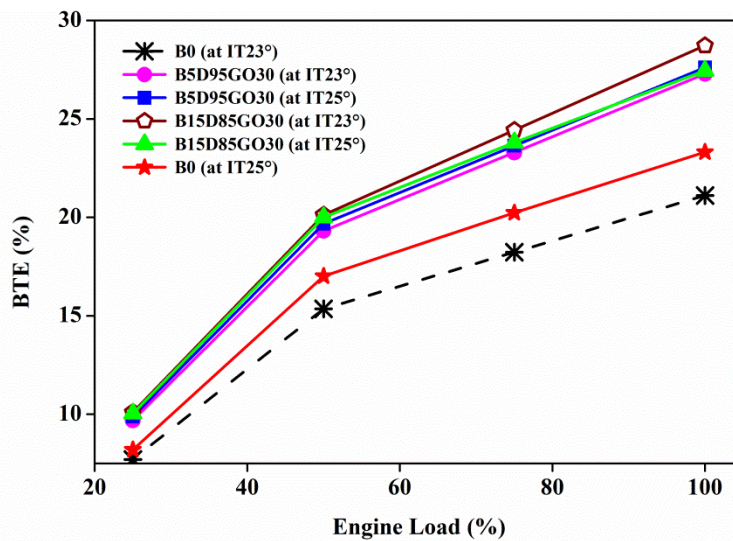
270 Fig. 5 depicts the variation of BTE with engine load for various GO-BDBs at IT23° & IT25°.  
271 It is inferred from the graph that BTE behaved harmoniously with load from 25 N to 100 N.  
272 In all load conditions, the B15D85GO30 fuel at IT23° gave the highest BTE results as  
273 compared to other fuels. The maximum BTE of about 28.73% was achieved by the blend  
274 B15D85GO30 at IT23°; whereas, for B5D95GO30 and B0 fuels, the BTE was found to be  
275 27.29% and 21.11% respectively at the same injection timing (Fig. 5). At IT25°, the BTE of  
276 B5D95GO30, B15D85GO30 & B0 was found to be 27.61%, 27.45% and 23.31%  
277 respectively. The reason behind the enhancement of BTE was due to the homogenous  
278 combination of the air-fuel which directly resulted in more heat release during combustion.  
279 Also, prolonged mixing time causes slow combustion [50–52]. Summarily, GO-BDBs gave  
280 better BTE results as compared to B0 at IT23° and IT25°.



281

282

Fig. 4. BSFC vs. engine load at various injection timings



283

284

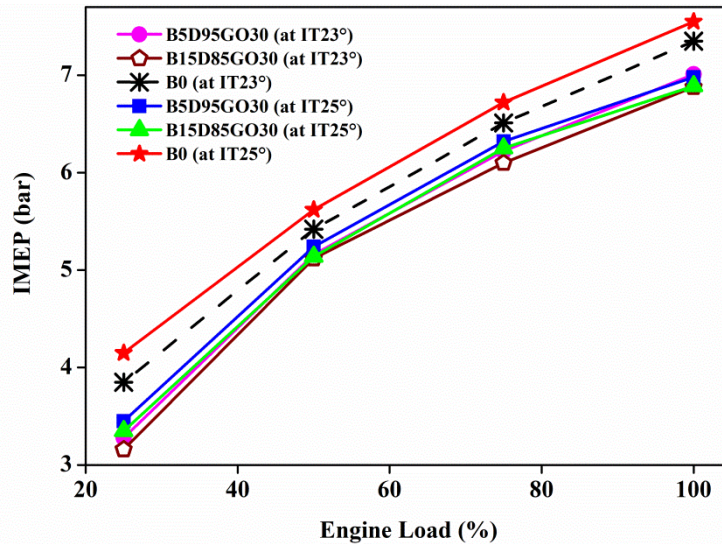
Fig. 5. BTE as a function of the injection timing at various loads

### 285 3.3.3. Indicated Mean Effective Pressure (IMEP)

286 The IMEP of the blend B15D85GO30 was observed to be low at both injection timings (Fig.  
 287 6). At partial load condition, the blend B15D85GO30 showed lower IMEP than other fuels.

288 The B15D95GO30 had 9.5% lower IMEP at IT25° & 6.4% lower at IT23° as compared to the  
 289 fossil diesel at maximum load. On the other hand, at IT23°, the IMEP of B5D95GO30 and  
 290 B15D85GO30 were 4.6% and 6.3% lower than pure diesel (B0) at full load condition;  
 291 whereas, at IT25°, they were decreased by 7.5% and 8.7% respectively.





292

293

Fig. 6. IMEP as a function of the injection timing

294

Thus, it is summarized that an increase in engine load led to an increase in IMEP for all GO-BDBs and pure diesel at both injection timings. Also, it was inferred that at both injection timings (IT23° and IT25°), the IMEP of GO-BDBs was lower than pure diesel.

297

### 3.3.4. Indicated Thermal Efficiency (ITE)

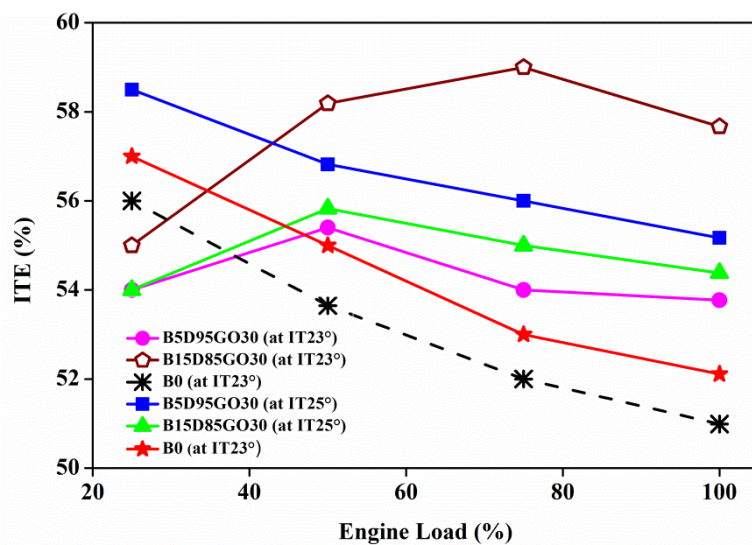
298

The variation of ITE at various injection timing for GO-BDBs is shown in Fig. 7. It was inferred that the ITE of B0 fuel gradually reduced for both injection timings. At higher load conditions, the ITE of B15D85GO30 at IT23° gave better results as compared to other fuels. The maximum ITE of 57.67% was achieved by the B15D85GO30 at IT23° (Fig. 7).

299

300

301



302

303

Fig. 7. ITE results as a function of engine load and injection timing

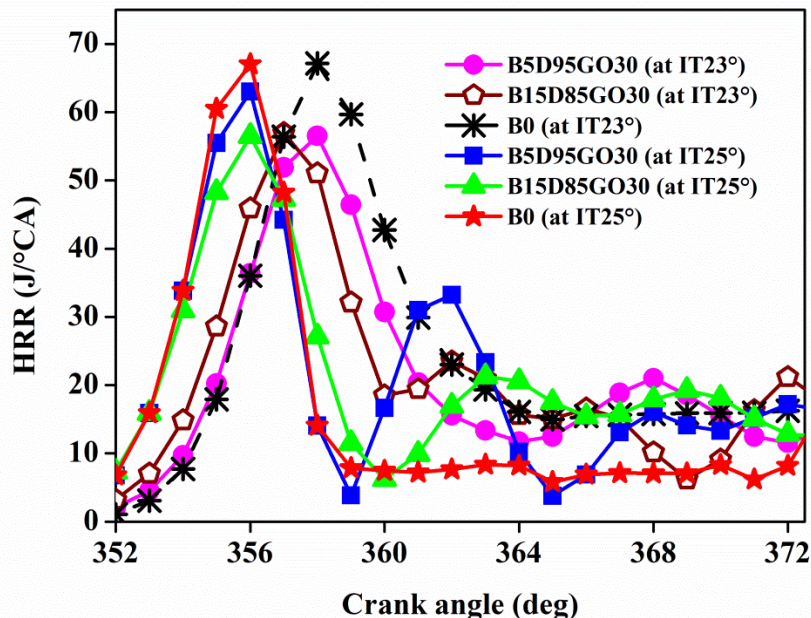


304 At IT23°, the maximum ITE of the B5D95GO30 and B0 fuels were found to be 53.77% and  
 305 50.99% respectively. Furthermore, at IT25°, the ITE of B5D95GO30, B15D85GO30 and B0  
 306 were found to be 55.17%, 54.38% and 52.11% respectively. The reason behind the ITE  
 307 improvement was due to the properties such as density, viscosity and lower compressibility  
 308 of GO-BDB's [53–55]. Summarily, the GO-BDBs gave better ITE results compared to pure  
 309 diesel at both IT23° and IT25°.

### 310 3.4. Combustion characteristics of nano-additive blends

#### 311 3.4.1. Heat release rate (HRR)

312 The variation in HRR of nanoparticle enhanced BDBs at IT23° and IT25° is depicted in Fig.  
 313 8. The peak HRRs of B15D85GO30 and B5D95GO30 fuels were found to be lower than that  
 314 of B0 fuel for both injection timings. At IT23°, the peak HRRs of B5D95GO30 and  
 315 B15D85GO30 fuels were 64 J/°CA and 55 J/°CA respectively. It was inferred that except  
 316 B5D95GO30 (at IT25°) and B0 (at IT25° & IT23°) fuels; all the other fuels liberated  
 317 approximately an equal amount of peak HRRs at both injection timings (Fig. 8). The start of  
 318 the combustion was advanced for all the GO-BDBs at IT25° and IT23° due to rich mixture in  
 319 the premixed ignition span and diffused combustion at the rest of the span [43,56].



320

321 Fig. 8. The HRR at full load and at various injection timings

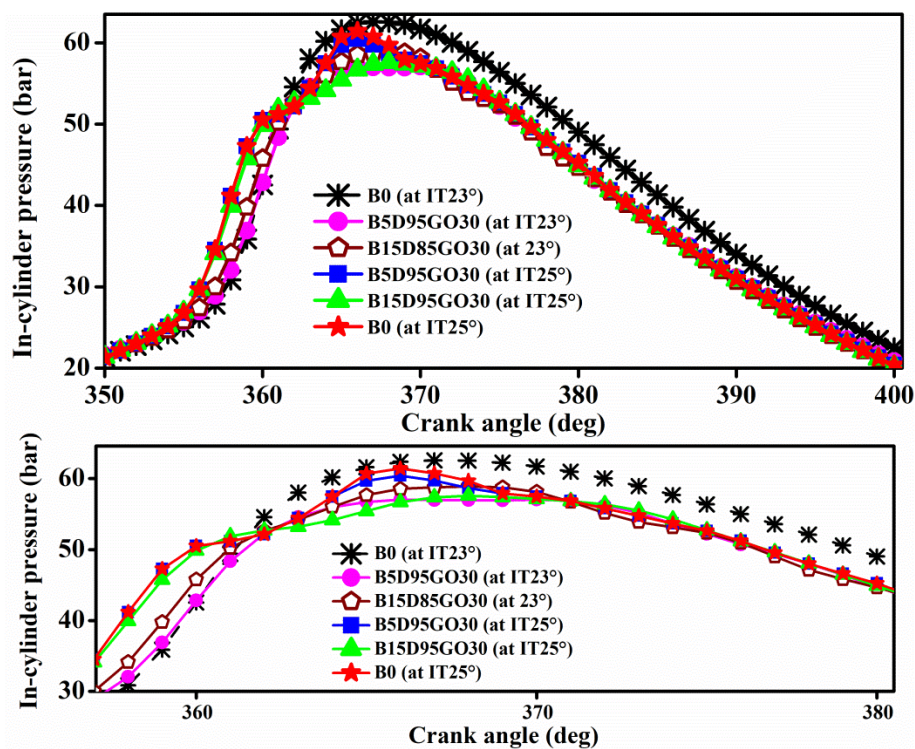
322 3.4.2. In-cylinder pressure

323 The in-cylinder pressures for GO-BDBs at full load (at IT23° and IT25°) is shown in Fig. 9.  
324 The peak in-cylinder pressure of B0, B5D85GO30 and B15D85GO30 was found to be 65  
325 bar, 56 bar and 59 bar respectively at IT23°. On the other hand, at IT25°, the peak in-cylinder  
326 pressures for B5D85GO30, B15D85GO30 and B0 were found to be 61 bar, 58 bar and 63 bar  
327 respectively (Fig. 9). The reason behind this variation was believed to be increased specific  
328 gravity of the BDB's when enhanced with GO nano-additives. Also, advancing the injection  
329 timings shorten the ignition delay and increase in the rate of fuel burning in the diffusion  
330 combustion phase are the dominating reasons to achieve lower combustion in-cylinder  
331 pressure with less knocking [28,57–61].

332 3.5. Exhaust gas emission characteristics

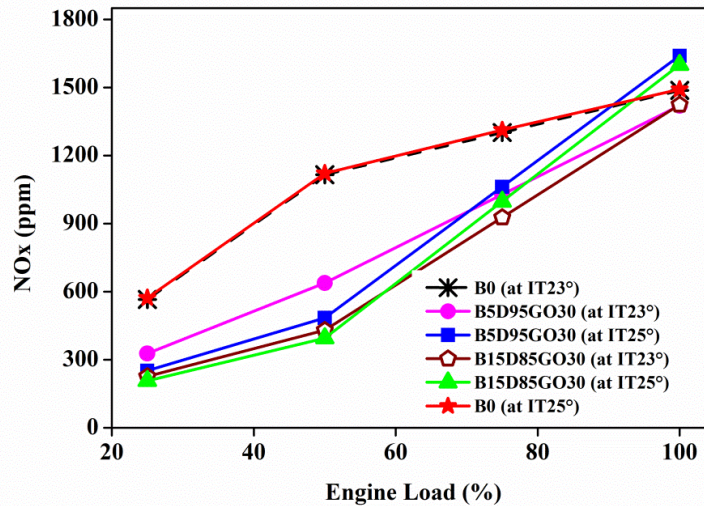
333 3.5.1. NOx gas emission

334 The NOx emission characteristics of the GO-BDBs at IT23° and IT25° are shown in Fig. 10.  
335 In general, NOx emission was found to be lower for nano-additive blends than pure diesel  
336 (Fig. 10). However, at maximum load with IT25°, the NOx emission of B15D85GO30 fuel  
337 was higher than fossil diesel.



338

339 Fig. 9. In-cylinder pressure as a function of injection timing



340

341

Fig. 10. NOx gas emission at various engine load and injection timing

342

343

344

345

346

347

348

349

350

351

At partial load condition and with IT23°, B5D95GO30 and B15D85GO30 blends emitted 42.8% and 61.4% lower NOx emission as compared to fossil diesel. Whereas, at peak load condition, the decrement percentage corresponds to 4.2% and 4.5% respectively for B5D95GO30 and B15D85GO30 blends as compared to diesel. Furthermore, it was observed that at part load condition, the NOx emissions of B5D95GO30 and B15D85GO30 blends were decreased by 56.8% and 64.7% respectively. The B5D95GO30 blend gave the lowest NOx gas emission both at IT23° and IT25° (Fig. 10). This NOx emission variation may be attributed due to premixed charge temperature during uncontrolled combustion zone and higher heat release rates [62–65]. Summarily, GO-BDBs gave lesser NOx emission as compared to pure diesel owing to the proper impregnation of GO additives.

352

### 3.5.2. Hydrocarbon (HC) emission

353

354

355

356

357

358

359

360

361

The HC emission of GO-BDBs at various injection timings is shown in Fig. 11. For pure diesel, at IT23° and IT25°, the rate of HC gas emission was increased as the engine load increased from 25% to 100% (Fig. 11). Furthermore, pure diesel emitted the same amount of HC at all loads at both injection timings, they were also higher than those obtained for nano-additive blends. Interestingly, the HC emission of GO-BDBs at IT23° was found to be lower as compared to the HC emission found at IT25°. At 50% load, and at IT25°, both GO-BDBs released almost the same amount of HC gas. It was also observed that at maximum load, the B15D85GO30 blend emitted about 50% lower HC emission when compared to the HC emission obtained for the pure diesel.

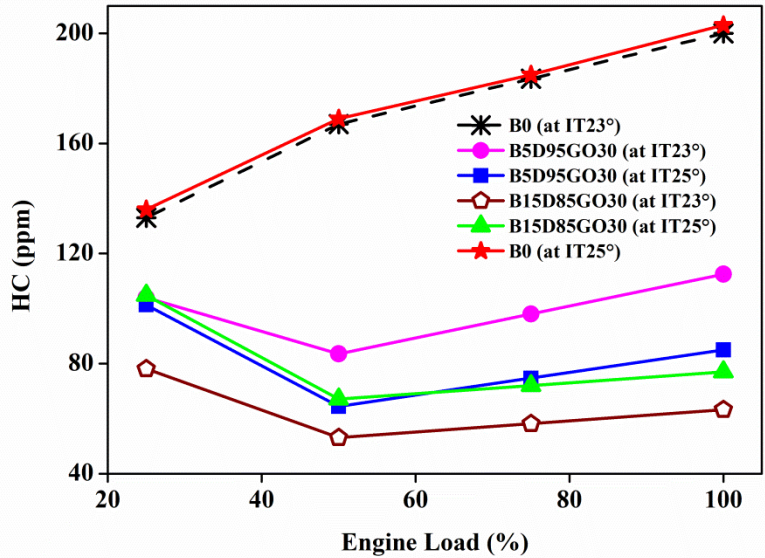


Fig. 11. HC emission as a function of engine load and injection timing

The HC emissions were lower for GO-BDBs as compared to diesel for all injection timings and loads due to the increase in gas temperature and higher oxygen content in GO-BDBs in comparison with conventional diesel. Nano-additives increases the rate of evaporation and cylinder temperature with improved mixing of air-fuel ratio leading to better oxidation and complete combustion process [66,67].

### 3.5.3. CO<sub>2</sub> emission

The CO<sub>2</sub> emission of the GO-BDBs at various engine loads and injection timing is shown in Fig. 12. Pure diesel emitted more CO<sub>2</sub> at both injection timings (IT23° and IT25°) as compared to GO-BDBs. In general, the CO<sub>2</sub> emission increased with the increase of engine load. The B15D85GO30 blend at IT23° gave the lowest CO<sub>2</sub> gas emission. Advancing the injection timing gave slightly lower CO<sub>2</sub> gas emissions for GO-BDBs (Fig. 12); this was happened due to the better premixing of air-fuel mixture providing sufficient time for the oxidation process to occur inside the cylinder [68,69].

### 3.5.4. Exhaust gas temperature (EGT)

Fig. 13 shows the EGT at various loads and injection timings. In general, the EGT was increased with the increase of engine loads. Pure diesel gave higher EGT as compared to GO-BDBs at both injection timings (Fig. 13). It was also observed that at any engine load and for all fuel blends, advancing the injection timings increased the EGT.



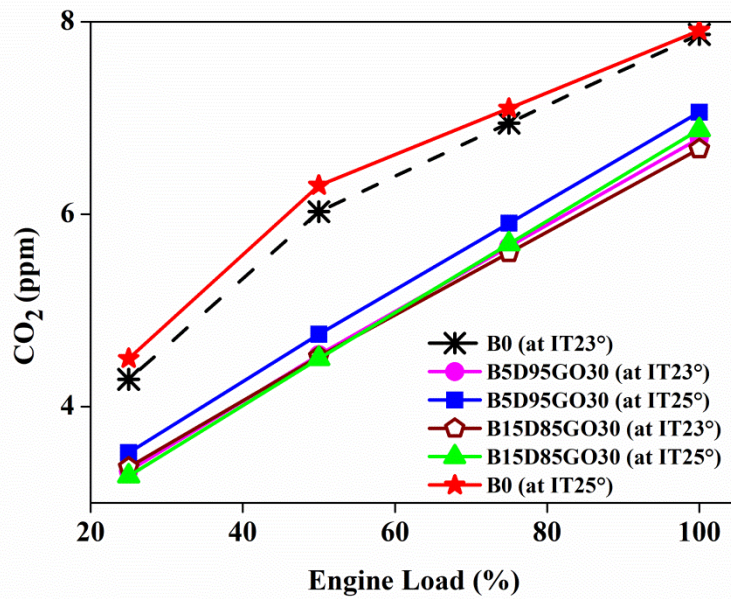


Fig. 12. CO<sub>2</sub> gas emission at various loads and injection timings

382

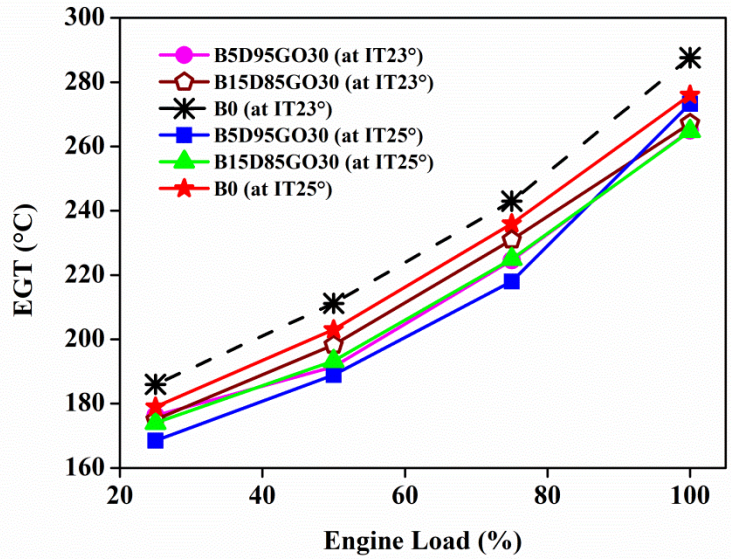
383

384 Furthermore, it was inferred that at full load and at IT23°, the EGT of B5D95GO30 and  
 385 B15D85GO30 were 22.7°C and 20.4°C lower as compared to pure diesel. Whereas at IT25°,  
 386 the EGT of B5D95GO30 and B15D85GO30 was 2.8°C and 11.3°C lower than pure diesel.  
 387 At partial load conditions, the differences in the EGT of GO-BDBs were not significant.  
 388 Overall, the EGT of B5D95GO30 and B15D85GO30 are 14-20°C and 9.7-13°C lower than  
 389 pure diesel at both injection timings. This may be due to the reason that the cetane numbers  
 390 of all GO-BDBs are lower as compared to fossil diesel (Table 6) and hence the ignition  
 391 delays for all these blends are relatively higher as compared to pure diesel [70]. Summarily,  
 392 GO-BDBs at IT25° gave lower EGT as compared to B0 fuel, the findings were supported by  
 393 the literature [71,72].

### 394 3.5.5 CO gas emission

395 The CO emission of the nano-additive blends was found to dwindle as the engine load  
 396 increased from 25% to 100% at both IT23° and IT25° (Fig. 14). At minimum loads, the CO  
 397 emission of pure diesel was lower than nano-additive blends. At full load, the GO-BDBs  
 398 emitted almost a similar amount of CO emissions. At partial loads, the CO emissions of the  
 399 B5D95GO30 at IT23° were observed to be lower as compared to the CO emissions at IT25°.  
 400 At IT23°, the B5D95GO30 and B15D85GO30 blends gave about 43% and 41.8% lower CO  
 401 emissions as compared to pure diesel. On the other hand, at IT25°, compared to pure diesel

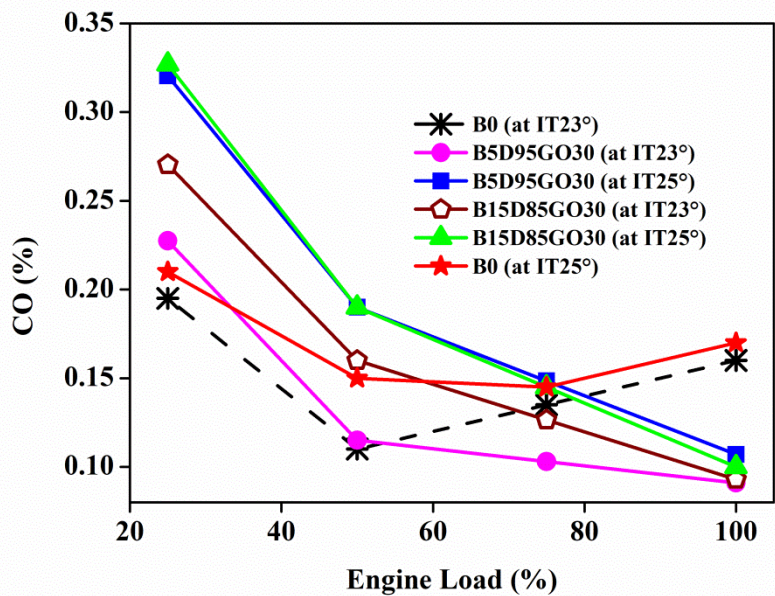
402 the CO emission was reduced by 37% and 41.17% for B5D95GO30 and B15D85GO30  
 403 blends respectively. Similar findings were found in the literature [71,73].



404

405

Fig. 13. EGT of tested fuels at various loads



406

407

Fig. 14. CO gas emissions at various loads and injection timings

408

409

410 **3.6. Potential application and recommendation for future work**

411 Owing to the size and thermo-physical properties of nanoparticles, they are widely used in  
412 bioscience, medical and engineering applications including robotics, automobile, solar  
413 collectors and desalination. The nanocomposites improved the stability, combustion and  
414 performance characteristics, with reduced emissions when blended with virgin biodiesel. This  
415 extends its potential application in the transportation sector as a direct substitute for diesel  
416 fuel. The blending of renewable fuel with pure diesel has been commissioned in various  
417 countries including the UK and India. The NBDB can also be used in railways as a substitute  
418 for virgin fuels. In 2007, The British Royal Train was operated with 100% biodiesel fuel  
419 (biodiesel was supplied by Green Fuels Ltd, UK.).

420 In addition to this, biodiesel outspreads its application in the aviation industry. In 2011,  
421 United Airlines (Eco-skies Boeing 737-800) reported that their first aviation flight was  
422 operated on biofuel blend with 40% biofuel and 60% petroleum-derived jet fuels. So, when  
423 NBDB is implemented in these sectors, the performance and combustion characteristics of  
424 the engines increases further with the reduced emission paving a green environment [74–76].

425 In addition, nanoparticle enhanced biodiesel could be used as a heating fuel (heating oil +  
426 nano-biofuel) in boilers (oil-fired boilers). Furthermore, NBDB can also be used in diesel  
427 generators to reduce environmental pollution. The biodiesel has the potential of producing  
428 78% less CO<sub>2</sub> emission as compared to fossil diesel [77,78] and this figure can further be  
429 reduced if NBDB is used. If traditional fuels are completely replaced with biodiesel and  
430 NBDBs, there will be a significant reduction in the emission of sulphur oxides, CO<sub>2</sub> and PM.  
431 Due to better buoyancy property, the NBDB fuels are used in shorelines to clean up the oil  
432 spills and to dissolve the crude oil through a single coating spraying process [75,79]. From  
433 the above applications, it is generally inferred that it is essential to bridge this outcome with  
434 other commercial end-users by integrating with various applications, thus reducing the  
435 reliance on petroleum products and to pave a better green environment for the future  
436 generation.

437 Future research can be focussed on (i) durability test of GO-biodiesel-diesel blends by  
438 conducting long hour engine operation and assessment of various engine components, (ii)  
439 implementing nano-additive blends for micro-algae species and immobilization of enzymes  
440 with the behavioural variations of a diesel engine, and (iii) in-depth characterisation of the

441 blends based on size, range, distribution and clustering should be enabled with respect  
442 nanoparticles and various biodiesel blends.

443

#### 444 **4. Conclusions**

445 Homogeneous graphene oxide - biodiesel - diesel blends (GO-BDB) were prepared and tested  
446 in a single-cylinder compression ignition engine. Macroscopic characterisations' were  
447 performed to confirm the presence of GO in the nano-additive blends. Fuel properties were  
448 measured. The injection timings and engine loads were varied. Engine performance,  
449 combustion and emission characteristics of the nano-additive blends were investigated and  
450 compared with pure diesel.

451

452 The findings of the study are summarized below:

453

454 (i) Compared to pure diesel, the flash point temperature, kinematic viscosity and density of  
455 the nano-additive blends were increased. On the other hand, the heating values and cetane  
456 number of the GO blends were reduced as compared to pure diesel.

457

458 (ii) At injection timing of 23°bTDC, brake specific fuel consumption, brake thermal  
459 efficiency, indicated mean effective pressure and indicated thermal efficiency of GO-BDBs  
460 were significantly improved as compared to pure diesel. At maximum load, the BSFC of the  
461 blend B5D95GO30 was found to be 13.5% and 11.5% lower than pure diesel at IT23° and  
462 IT25° respectively. The BTE and ITE of B15D95GO30 & B5D85GO30 blends were 7.62%  
463 & 5.8% and 6.8% & 4% higher than pure diesel at IT23° and at maximum load condition.  
464 However, better ITE was achieved at IT25° as compared to IT23°. At full load condition and  
465 at IT25°, the B15D85GO30 fuel gave lowest indicated mean effective pressure and was found  
466 to be 9.5% lower than pure diesel.

467

468 (iii) At maximum load, the heat release rates of nano-additive blends were found to be lower  
469 than the pure diesel at both injection timings of IT25° and IT23°. The peak in-cylinder  
470 pressures of B5D95GO30 at IT23° and B15D85GO30 at IT25° yielded minimum values as  
471 compared to pure diesel at maximum load conditions.

472

473 (iv) In general, the exhaust gas temperatures, CO<sub>2</sub>, HC, and NO<sub>x</sub> emissions of the nano-  
474 additive blends were decreased at all loads and at both injection timings. In addition, the HC,  
475 NO<sub>x</sub>, CO<sub>2</sub> emissions were found to be significantly reduced for GO blends as compared to  
476 pure diesel at injection timing of 23° bTDC.



477 The study concluded that B15D85GO30 at IT23° gave optimum performance, combustion  
478 and emission characteristics when compared to other fuels considered for experimentation.  
479 Hence B15D85GO30 is suggested as a suitable blend for use in the diesel engine.

480

481

## 482 **References**

- 483 [1] S.M. Palash, M.A. Kalam, H.H. Masjuki, B.M. Masum, I.M. Rizwanul Fattah, M.  
484 Mofijur, Impacts of biodiesel combustion on NO<sub>x</sub> emissions and their reduction  
485 approaches, *Renew. Sustain. Energy Rev.* 23 (2013) 473–490.  
486 doi:10.1016/J.RSER.2013.03.003.
- 487 [2] A. Demirbas, Progress and recent trends in biodiesel fuels, *Energy Convers. Manag.*  
488 50 (2009) 14–34. doi:10.1016/J.ENCONMAN.2008.09.001.
- 489 [3] İ. Çelikten, E. Mutlu, H. Solmaz, Variation of performance and emission  
490 characteristics of a diesel engine fueled with diesel, rapeseed oil and hazelnut oil  
491 methyl ester blends, *Renew. Energy.* 48 (2012) 122–126.  
492 doi:10.1016/J.RENENE.2012.04.040.
- 493 [4] M. Mofijur, H.H. Masjuki, M.A. Kalam, A.E. Atabani, M. Shahabuddin, S.M. Palash,  
494 M.A. Hazrat, Effect of biodiesel from various feedstocks on combustion  
495 characteristics, engine durability and materials compatibility: A review, *Renew.*  
496 *Sustain. Energy Rev.* 28 (2013) 441–455. doi:10.1016/J.RSER.2013.07.051.
- 497 [5] A. Kadarohman, Hernani, I. Rohman, R. Kusriani, R.M. Astuti, Combustion  
498 characteristics of diesel fuel on one cylinder diesel engine using clove oil, eugenol, and  
499 eugenyl acetate as fuel bio-additives, *Fuel.* 98 (2012) 73–79.  
500 doi:10.1016/J.FUEL.2012.03.037.
- 501 [6] V. Saxena, N. Kumar, V.K. Saxena, A comprehensive review on combustion and  
502 stability aspects of metal nanoparticles and its additive effect on diesel and biodiesel  
503 fuelled C.I. engine, *Renew. Sustain. Energy Rev.* 70 (2017) 563–588.  
504 doi:10.1016/j.rser.2016.11.067.
- 505 [7] C.S. Aalam, C.G. Saravanan, M. Kannan, Experimental investigations on a CRDI  
506 system assisted diesel engine fuelled with aluminium oxide nanoparticles blended  
507 biodiesel, *Alexandria Eng. J.* 54 (2015) 351–358. doi:10.1016/J.AEJ.2015.04.009.
- 508 [8] P. Appavu, M. Venkata Ramanan, Study of emission characteristics of a diesel engine  
509 using cerium oxide nanoparticle blended pongamia methyl ester, *Int. J. Ambient*

- 510 Energy. (2018) 1–4. doi:10.1080/01430750.2018.1477063.
- 511 [9] C. Srinidhi, A. Madhusudhan, S.V. Channapattana, Effect of NiO nanoparticles on  
512 performance and emission characteristics at various injection timings using biodiesel-  
513 diesel blends, *Fuel*. 235 (2019) 185–193. doi:10.1016/J.FUEL.2018.07.067.
- 514 [10] M.E.M. Soudagar, N.-N. Nik-Ghazali, M.A. Kalam, I.A. Badruddin, N.R.  
515 Banapurmath, T.M. Yunus Khan, M.N. Bashir, N. Akram, R. Farade, A. Afzal, The  
516 effects of graphene oxide nanoparticle additive stably dispersed in dairy scum oil  
517 biodiesel-diesel fuel blend on CI engine: performance, emission and combustion  
518 characteristics, *Fuel*. 257 (2019) 116015. doi:10.1016/J.FUEL.2019.116015.
- 519 [11] A. Fayyazbakhsh, V. Pirouzfard, Investigating the influence of additives-fuel on diesel  
520 engine performance and emissions: Analytical modeling and experimental validation,  
521 *Fuel*. 171 (2016) 167–177. doi:10.1016/J.FUEL.2015.12.028.
- 522 [12] M.E.M. Soudagar, N.-N. Nik-Ghazali, M. Abul Kalam, I.A. Badruddin, N.R.  
523 Banapurmath, N. Akram, The effect of nano-additives in diesel-biodiesel fuel blends:  
524 A comprehensive review on stability, engine performance and emission characteristics,  
525 *Energy Convers. Manag.* 178 (2018) 146–177.  
526 doi:10.1016/J.ENCONMAN.2018.10.019.
- 527 [13] S. Nagaraja, M. Sakthivel, R. Sudhakaran, Comparative study of the combustion,  
528 performance, and emission characteristics of a variable compression ratio engine  
529 fuelled with diesel, corn oil methyl ester, and palm oil methyl ester, *J. Renew. Sustain.*  
530 *Energy*. 4 (2012) 063122. doi:10.1063/1.4768543.
- 531 [14] A. Fayyazbakhsh, V. Pirouzfard, Comprehensive overview on diesel additives to reduce  
532 emissions, enhance fuel properties and improve engine performance, *Renew. Sustain.*  
533 *Energy Rev.* 74 (2017) 891–901. doi:10.1016/J.RSER.2017.03.046.
- 534 [15] Ü. Ağbulut, M. Karagöz, S. Sarıdemir, A. Öztürk, Impact of various metal-oxide based  
535 nanoparticles and biodiesel blends on the combustion, performance, emission,  
536 vibration and noise characteristics of a CI engine, *Fuel*. 270 (2020) 117521.  
537 doi:10.1016/j.fuel.2020.117521.
- 538 [16] M.S. Gad, S. Jayaraj, A comparative study on the effect of nano-additives on the  
539 performance and emissions of a diesel engine run on Jatropha biodiesel, *Fuel*. 267  
540 (2020) 117168. doi:10.1016/j.fuel.2020.117168.
- 541 [17] M.T. Chaichan, A.A.H. Kadhum, A.A. Al-Amiery, Novel technique for enhancement  
542 of diesel fuel: Impact of aqueous alumina nano-fluid on engine's performance and

- 543 emissions, *Case Stud. Therm. Eng.* 10 (2017) 611–620.  
544 doi:10.1016/j.csite.2017.11.006.
- 545 [18] M.E.M. Soudagar, N.N. Nik-Ghazali, M.A. Kalam, I.A. Badruddin, N.R.  
546 Banapurmath, M.A. Bin Ali, S. Kamangar, H.M. Cho, N. Akram, An investigation on  
547 the influence of aluminium oxide nano-additive and honge oil methyl ester on engine  
548 performance, combustion and emission characteristics, *Renew. Energy*. 146 (2020)  
549 2291–2307. doi:10.1016/j.renene.2019.08.025.
- 550 [19] R.N. Mehta, M. Chakraborty, P.A. Parikh, Nanofuels: Combustion, engine  
551 performance and emissions, *Fuel*. 120 (2014) 91–97.  
552 doi:10.1016/J.FUEL.2013.12.008.
- 553 [20] A. Prabu, Nanoparticles as additive in biodiesel on the working characteristics of a DI  
554 diesel engine, *Ain Shams Eng. J.* 9 (2018) 2343–2349.  
555 doi:10.1016/J.ASEJ.2017.04.004.
- 556 [21] A. Hossain, A. Hussain, Impact of Nanoadditives on the Performance and Combustion  
557 Characteristics of Neat Jatropha Biodiesel, *Energies*. 12 (2019) 921.  
558 doi:10.3390/en12050921.
- 559 [22] P.M. Shameer, K. Ramesh, Assessment on the consequences of injection timing and  
560 injection pressure on combustion characteristics of sustainable biodiesel fuelled  
561 engine, *Renew. Sustain. Energy Rev.* 81 (2018) 45–61. doi:10.1016/j.rser.2017.07.048.
- 562 [23] S. Manigandan, P. Gunasekar, J. Devipriya, S. Nithya, Emission and injection  
563 characteristics of corn biodiesel blends in diesel engine, *Fuel*. 235 (2019) 723–735.  
564 doi:10.1016/J.FUEL.2018.08.071.
- 565 [24] A. Yaşar, A. Keskin, Ş. Yıldızhan, E. Uludamar, Emission and vibration analysis of  
566 diesel engine fuelled diesel fuel containing metallic based nanoparticles, *Fuel*. 239  
567 (2019) 1224–1230. doi:10.1016/J.FUEL.2018.11.113.
- 568 [25] S. Akram, M.W. Mumtaz, M. Danish, H. Mukhtar, A. Irfan, S.A. Raza, Z. Wang, M.  
569 Arshad, Impact of cerium oxide and cerium composite oxide as nano additives on the  
570 gaseous exhaust emission profile of waste cooking oil based biodiesel at full engine  
571 load conditions, *Renew. Energy*. 143 (2019) 898–905.  
572 doi:10.1016/j.renene.2019.05.025.
- 573 [26] H. Venu, L. Subramani, V.D. Raju, Emission reduction in a DI diesel engine using  
574 exhaust gas recirculation (EGR) of palm biodiesel blended with TiO<sub>2</sub> nano additives,  
575 *Renew. Energy*. 140 (2019) 245–263. doi:10.1016/j.renene.2019.03.078.

- 576 [27] A. Heidari-Maleni, T. Mesri Gundoshmian, A. Jahanbakhshi, B. Ghobadian,  
577 Performance improvement and exhaust emissions reduction in diesel engine through  
578 the use of graphene quantum dot (GQD) nanoparticles and ethanol-biodiesel blends,  
579 *Fuel*. 267 (2020) 117116. doi:10.1016/j.fuel.2020.117116.
- 580 [28] A.I. El-Seesy, A.K. Abdel-Rahman, M. Bady, S. Ookawara, Performance, combustion,  
581 and emission characteristics of a diesel engine fueled by biodiesel-diesel mixtures with  
582 multi-walled carbon nanotubes additives, *Energy Convers. Manag.* 135 (2017) 373–  
583 393. doi:10.1016/J.ENCONMAN.2016.12.090.
- 584 [29] S.S. Hoseini, G. Najafi, B. Ghobadian, M.T. Ebadi, R. Mamat, T. Yusaf, Biodiesels  
585 from three feedstock: The effect of graphene oxide (GO) nanoparticles diesel engine  
586 parameters fuelled with biodiesel, *Renew. Energy*. 145 (2020) 190–201.  
587 doi:10.1016/J.RENENE.2019.06.020.
- 588 [30] A.I. EL-Seesy, H. Hassan, S. Ookawara, Performance, combustion, and emission  
589 characteristics of a diesel engine fueled with Jatropha methyl ester and graphene oxide  
590 additives, *Energy Convers. Manag.* 166 (2018) 674–686.  
591 doi:10.1016/J.ENCONMAN.2018.04.049.
- 592 [31] A.I. El-Seesy, H. Hassan, S. Ookawara, Effects of graphene nanoplatelet addition to  
593 jatropha Biodiesel–Diesel mixture on the performance and emission characteristics of  
594 a diesel engine, *Energy*. 147 (2018) 1129–1152. doi:10.1016/j.energy.2018.01.108.
- 595 [32] A.I. EL-Seesy, H. Hassan, Investigation of the effect of adding graphene oxide,  
596 graphene nanoplatelet, and multiwalled carbon nanotube additives with n-butanol-  
597 Jatropha methyl ester on a diesel engine performance, *Renew. Energy*. 132 (2019)  
598 558–574. doi:10.1016/j.renene.2018.08.026.
- 599 [33] S.S. Hoseini, G. Najafi, B. Ghobadian, R. Mamat, M.T. Ebadi, T. Yusaf, Novel  
600 environmentally friendly fuel: The effects of nanographene oxide additives on the  
601 performance and emission characteristics of diesel engines fuelled with *Ailanthus*  
602 *altissima* biodiesel, *Renew. Energy*. 125 (2018) 283–294.  
603 doi:10.1016/j.renene.2018.02.104.
- 604 [34] N.A. Ihoeghian, M.A. Usman, Exergetic evaluation of biodiesel production from rice  
605 bran oil using heterogeneous catalyst, *J. King Saud Univ. - Eng. Sci.* 32 (2020) 101–  
606 107. doi:10.1016/j.jksues.2018.11.007.
- 607 [35] V.C. Pandey, K. Singh, J.S. Singh, A. Kumar, B. Singh, R.P. Singh, *Jatropha curcas*: A  
608 potential biofuel plant for sustainable environmental development, *Renew. Sustain.*

- 609 Energy Rev. 16 (2012) 2870–2883. doi:10.1016/j.rser.2012.02.004.
- 610 [36] A. Demirbas, A. Bafail, W. Ahmad, M. Sheikh, Biodiesel production from non-edible  
611 plant oils, Energy Explor. Exploit. 34 (2016) 290–318.  
612 doi:10.1177/0144598716630166.
- 613 [37] S. Nagaraja, K. Soorya Prakash, R. Sudhakaran, M. Sathish Kumar, Investigation on  
614 the emission quality, performance and combustion characteristics of the compression  
615 ignition engine fueled with environmental friendly corn oil methyl ester – Diesel  
616 blends, Ecotoxicol. Environ. Saf. 134 (2016) 455–461.  
617 doi:10.1016/J.ECOENV.2016.01.023.
- 618 [38] S. Nagaraja, S. Praveen, R. Prakash, J. Sriram, Impact of compression ratio analysis in  
619 waste cooking oil biodiesels–diesel blends as fuel, Int. J. Ambient Energy. (2018).  
620 doi:10.1080/01430750.2018.1490350.
- 621 [39] T. Shaafi, K. Sairam, A. Gopinath, G. Kumaresan, R. Velraj, Effect of dispersion of  
622 various nanoadditives on the performance and emission characteristics of a CI engine  
623 fuelled with diesel, biodiesel and blends—A review, Renew. Sustain. Energy Rev. 49  
624 (2015) 563–573. doi:10.1016/j.rser.2015.04.086.
- 625 [40] S. Witharana, C. Hodges, D. Xu, X. Lai, Y. Ding, Aggregation and settling in aqueous  
626 polydisperse alumina nanoparticle suspensions, J. Nanoparticle Res. 14 (2012) 1–11.  
627 doi:10.1007/s11051-012-0851-3.
- 628 [41] M.F. Zawrah, R.M. Khattab, L.G. Girgis, H. El Daidamony, R.E. Abdel Aziz, Stability  
629 and electrical conductivity of water-base Al<sub>2</sub>O<sub>3</sub> nanofluids for different applications,  
630 HBRC J. 12 (2016) 227–234. doi:10.1016/j.hbrcj.2014.12.001.
- 631 [42] S.K. Das, S.U.S. Choi, H.E. Patel, Heat Transfer in Nanofluids—A Review, Heat  
632 Transf. Eng. 27 (2006) 3–19. doi:10.1080/01457630600904593.
- 633 [43] M.-S. Liu, M. Ching-Cheng Lin, I.-T. Huang, C.-C. Wang, Enhancement of thermal  
634 conductivity with carbon nanotube for nanofluids, Int. Commun. Heat Mass Transf. 32  
635 (2005) 1202–1210. doi:10.1016/J.ICHEATMASSTRANSFER.2005.05.005.
- 636 [44] D. Dsilva Winfred Rufuss, S. Iniyan, L. Suganthi, P.A. Davies, Low mass fraction  
637 impregnation with graphene oxide (GO) enhances thermo-physical properties of  
638 paraffin for heat storage applications, Thermochim. Acta. 655 (2017) 226–233.  
639 doi:10.1016/j.tca.2017.07.005.
- 640 [45] I. Khan, K. Saeed, I. Khan, Nanoparticles: Properties, applications and toxicities, Arab.  
641 J. Chem. 12 (2019) 908–931. doi:10.1016/j.arabjc.2017.05.011.

- 642 [46] W. Zhu, R. Esteban, A.G. Borisov, J.J. Baumberg, P. Nordlander, H.J. Lezec, J.  
643 Aizpurua, K.B. Crozier, Quantum mechanical effects in plasmonic structures with  
644 subnanometre gaps, *Nat. Commun.* 7 (2016) 1–14. doi:10.1038/ncomms11495.
- 645 [47] J. Jeevanandam, A. Barhoum, Y.S. Chan, A. Dufresne, M.K. Danquah, Review on  
646 nanoparticles and nanostructured materials: History, sources, toxicity and regulations,  
647 *Beilstein J. Nanotechnol.* 9 (2018) 1050–1074. doi:10.3762/bjnano.9.98.
- 648 [48] D. Dsilva Winfred Rufuss, L. Suganthi, S. Iniyar, P.A. Davies, Effects of  
649 nanoparticle-enhanced phase change material (NPCM) on solar still productivity, *J.*  
650 *Clean. Prod.* 192 (2018) 9–29. doi:10.1016/j.jclepro.2018.04.201.
- 651 [49] M. Mirzajanzadeh, M. Tabatabaei, M. Ardjmand, A. Rashidi, B. Ghobadian, M.  
652 Barkhi, M. Pazouki, A novel soluble nano-catalysts in diesel–biodiesel fuel blends to  
653 improve diesel engines performance and reduce exhaust emissions, *Fuel.* 139 (2015)  
654 374–382. doi:10.1016/J.FUEL.2014.09.008.
- 655 [50] M. Channappagoudra, K. Ramesh, G. Manavendra, Effect of injection timing on  
656 modified direct injection diesel engine performance operated with dairy scum biodiesel  
657 and Bio-CNG, *Renew. Energy.* 147 (2020) 1019–1032.  
658 doi:10.1016/J.RENENE.2019.09.070.
- 659 [51] V. Belagur, V. Reddy Phd, Influence of fuel injection rate on the performance,  
660 emission and combustion characteristics of di diesel engine running on calophyllum  
661 inophyllum linn oil (honne oil)/diesel fuel blend, in: *SAE Tech. Pap.*, SAE  
662 International, 2010. doi:10.4271/2010-01-1961.
- 663 [52] J. Hwang, D. Qi, Y. Jung, C. Bae, Effect of injection parameters on the combustion  
664 and emission characteristics in a common-rail direct injection diesel engine fueled with  
665 waste cooking oil biodiesel, *Renew. Energy.* 63 (2014) 9–17.  
666 doi:10.1016/J.RENENE.2013.08.051.
- 667 [53] A.N. Ozsezen, M. Canakci, C. Sayin, Effects of Biodiesel from Used Frying Palm Oil  
668 on the Performance, Injection, and Combustion Characteristics of an Indirect Injection  
669 Diesel Engine, *Energy & Fuels.* 22 (2008) 1297–1305. doi:10.1021/ef700447z.
- 670 [54] M. Canakci, J.H. Van Gerpen, Comparison of engine eformance and emissions for  
671 petroleum diesel fuel, yellow grease biodiesel, and soybean oil biodiesel, *Trans.*  
672 *ASAE.* 46 (n.d.) 937–944.
- 673 [55] A.N. Ozsezen, M. Canakci, A. Turkcan, C. Sayin, Performance and combustion  
674 characteristics of a DI diesel engine fueled with waste palm oil and canola oil methyl

- 675 esters, *Fuel*. 88 (2009) 629–636. doi:10.1016/J.FUEL.2008.09.023.
- 676 [56] Y. Hwang, J.K. Lee, C.H. Lee, Y.M. Jung, S.I. Cheong, C.G. Lee, B.C. Ku, S.P. Jang,  
677 Stability and thermal conductivity characteristics of nanofluids, *Thermochim. Acta*.  
678 455 (2007) 70–74. doi:10.1016/J.TCA.2006.11.036.
- 679 [57] A.F. Chen, M. Akmal Adzmi, A. Adam, M.F. Othman, M.K. Kamaruzzaman, A.G.  
680 Mrwan, Combustion characteristics, engine performances and emissions of a diesel  
681 engine using nanoparticle-diesel fuel blends with aluminium oxide, carbon nanotubes  
682 and silicon oxide, *Energy Convers. Manag.* 171 (2018) 461–477.  
683 doi:10.1016/J.ENCONMAN.2018.06.004.
- 684 [58] S.H. Hosseini, A. Taghizadeh-Alisaraei, B. Ghobadian, A. Abbaszadeh-Mayvan,  
685 Performance and emission characteristics of a CI engine fuelled with carbon nanotubes  
686 and diesel-biodiesel blends, *Renew. Energy*. 111 (2017) 201–213.  
687 doi:10.1016/J.RENENE.2017.04.013.
- 688 [59] M. Annamalai, B. Dhinesh, K. Nanthagopal, P. SivaramaKrishnan, J. Isaac  
689 JoshuaRamesh Lalvani, M. Parthasarathy, K. Annamalai, An assessment on  
690 performance, combustion and emission behavior of a diesel engine powered by ceria  
691 nanoparticle blended emulsified biofuel, *Energy Convers. Manag.* 123 (2016) 372–  
692 380. doi:10.1016/J.ENCONMAN.2016.06.062.
- 693 [60] H. Soukht Saraee, H. Taghavifar, S. Jafarmadar, Experimental and numerical  
694 consideration of the effect of CeO<sub>2</sub> nanoparticles on diesel engine performance and  
695 exhaust emission with the aid of artificial neural network, *Appl. Therm. Eng.* 113  
696 (2017) 663–672. doi:10.1016/J.APPLTHERMALENG.2016.11.044.
- 697 [61] L. Kumari, T. Zhang, G.H. Du, W.Z. Li, Q.W. Wang, A. Datye, K.H. Wu, Thermal  
698 properties of CNT-Alumina nanocomposites, *Compos. Sci. Technol.* 68 (2008) 2178–  
699 2183. doi:10.1016/J.COMPSCITECH.2008.04.001.
- 700 [62] G.H. Abd Alla, H.A. Soliman, O.A. Badr, M.F. Abd Rabbo, Effect of pilot fuel  
701 quantity on the performance of a dual fuel engine, *Energy Convers. Manag.* 41 (2000)  
702 559–572. doi:10.1016/S0196-8904(99)00124-7.
- 703 [63] T. Shaafi, R. Velraj, Influence of alumina nanoparticles, ethanol and isopropanol blend  
704 as additive with diesel–soybean biodiesel blend fuel: Combustion, engine performance  
705 and emissions, *Renew. Energy*. 80 (2015) 655–663.  
706 doi:10.1016/J.RENENE.2015.02.042.
- 707 [64] M. Roshith, O. George, M. Sajunulal Franc, M. Sachin, J. James, M.M. John, M.G.

- 708 Sebastian, An Experimental Analysis on Synergetic Effect of Multiple Nanoparticle  
709 Blended Diesel Fuel on CI Engine, *IJIRST-International J. Innov. Res. Sci. Technol.* 1  
710 (2015). [www.ijirst.org](http://www.ijirst.org) (accessed December 1, 2019).
- 711 [65] A.M.A. Attia, A.I. El-Seesy, H.M. El-Batsh, M.S. Shehata, Effects of Alumina  
712 Nanoparticles Additives Into Jojoba Methyl Ester-Diesel Mixture on Diesel Engine  
713 Performance, in: *ASME 2014 Int. Mech. Eng. Congr. Expo.*, ASME International,  
714 2014: pp. IMECE2014-39988, V06BT07A019; 10 pages. doi:10.1115/imece2014-  
715 39988.
- 716 [66] B.N. Rao, B.S. Prem Kumar, K.V. Kumar Reddy, Effect of CNG flow rate on the  
717 performance and emissions of a Mullite-coated diesel engine under dual-fuel mode,  
718 *Int. J. Ambient Energy.* 37 (2016) 589–596. doi:10.1080/01430750.2015.1023835.
- 719 [67] V. Sajith, C.B. Sobhan, G.P. Peterson, Experimental Investigations on the Effects of  
720 Cerium Oxide Nanoparticle Fuel Additives on Biodiesel, *Adv. Mech. Eng.* 2 (2010)  
721 581407. doi:10.1155/2010/581407.
- 722 [68] G. Vairamuthu, S. Sundarapandian, C. Kailasanathan, B. Thangagiri, Experimental  
723 investigation on the effects of cerium oxide nanoparticle on *Calophyllum inophyllum*  
724 (Punnai) biodiesel blended with diesel fuel in DI diesel engine modified by nozzle  
725 geometry, *J. Energy Inst.* 89 (2016) 668–682. doi:10.1016/J.JOIEI.2015.05.005.
- 726 [69] E. Khalife, M. Tabatabaei, B. Najafi, S.M. Mirsalim, A. Gharehghani, P. Mohammadi,  
727 M. Aghbashlo, A. Ghaffari, Z. Khounani, T. Roodbar Shojaei, M.A. Mohd Salleh, A  
728 novel emulsion fuel containing aqueous nano cerium oxide additive in diesel–biodiesel  
729 blends to improve diesel engines performance and reduce exhaust emissions: Part I –  
730 Experimental analysis, *Fuel.* 207 (2017) 741–750. doi:10.1016/J.FUEL.2017.06.033.
- 731 [70] W. Fan, M. Jia, Y. Chang, M. Xie, Understanding the relationship between cetane  
732 number and the ignition delay in shock tubes for different fuels based on a skeletal  
733 primary reference fuel (n-hexadecane/iso-cetane) mechanism, *Energy and Fuels.* 29  
734 (2015) 3413–3427. doi:10.1021/ef5028185.
- 735 [71] S. Kumar, P. Dinesha, I. Bran, Influence of nanoparticles on the performance and  
736 emission characteristics of a biodiesel fuelled engine: An experimental analysis,  
737 *Energy.* 140 (2017) 98–105. doi:10.1016/J.ENERGY.2017.08.079.
- 738 [72] J. Gardy, A. Hassanpour, X. Lai, M.H. Ahmed, M. Rehan, Biodiesel production from  
739 used cooking oil using a novel surface functionalised TiO<sub>2</sub> nano-catalyst, *Appl. Catal.*  
740 *B Environ.* 207 (2017) 297–310. doi:10.1016/J.APCATB.2017.01.080.



- 741 [73] A. Ranjan, S.S. Dawn, J. Jayaprabakar, N. Nirmala, K. Saikiran, S. Sai Sriram,  
742 Experimental investigation on effect of MgO nanoparticles on cold flow properties,  
743 performance, emission and combustion characteristics of waste cooking oil biodiesel,  
744 Fuel. 220 (2018) 780–791. doi:10.1016/J.FUEL.2018.02.057.
- 745 [74] A.K. Agarwal, Biofuels (alcohols and biodiesel) applications as fuels for internal  
746 combustion engines, Prog. Energy Combust. Sci. 33 (2007) 233–271.  
747 doi:10.1016/j.pecs.2006.08.003.
- 748 [75] D.F. McCay, J.J. Rowe, N. Whittier, S. Sankaranarayanan, D.S. Etkin, Estimation of  
749 potential impacts and natural resource damages of oil, J. Hazard. Mater. 107 (2004)  
750 11–25. doi:10.1016/j.jhazmat.2003.11.013.
- 751 [76] R.J. McDonald, Proceedings of the 2003 national oilheat research alliance technology  
752 symposium, Boston, Massachusetts, n.d.  
753 doi:<https://www.bnl.gov/isd/documents/25281.pdf>.
- 754 [77] K.S. Tyson, Biodiesel--Clean, Green Diesel Fuel: Great Fleet Fuel Gaining Popularity  
755 Rapidly, 2001. doi:<https://afdc.energy.gov/files/pdfs/30882.pdf>.
- 756 [78] A. Monyem, J. H. Van Gerpen, The effect of biodiesel oxidation on engine  
757 performance and emissions, Biomass and Bioenergy. 20 (2001) 317–325.  
758 doi:10.1016/S0961-9534(00)00095-7.
- 759 [79] P. Fernández-Álvarez, J. Vila, J.M. Garrido, M. Grifoll, G. Feijoo, J.M. Lema,  
760 Evaluation of biodiesel as bioremediation agent for the treatment of the shore affected  
761 by the heavy oil spill of the Prestige, J. Hazard. Mater. 147 (2007) 914–922.  
762 doi:10.1016/j.jhazmat.2007.01.135.  
763